

Development of an Optical Gyroscope for Ground Tilt Sensing in Advanced LIGO

Progress Report 2

Michelle Stephens
Mentors: Alastair Heptonstall and Peter King
August 3, 2009

Laser Interferometer Gravitational Wave Observatory
- LIGO -
California Institute of Technology
Massachusetts Institute of Technology

Abstract

The LIGO gravitational wave detectors are scheduled to undergo major upgrades, known as Advanced LIGO, to improve their sensitivity by a factor of ten. Low frequency isolation of LIGO's suspension systems from seismic noise is achieved actively using seismometers to feed forward to hydraulic actuators. The sensitivity of the seismometers to translations meets design specifications at detection band frequencies. As the interferometer length is altered by test mass motion at lower frequencies, however, there is a non-linear coupling of mirror motion to the output signal of the interferometer. Below approximately 10 Hz, coupling of ground tilt and rotation into the horizontal seismometer signal becomes problematic, and at lower frequencies the signal becomes dominated by tilt. Using a ground tilt sensor in parallel with the seismometers, it is possible to remove this component of the signal before driving the hydraulic stages. This sensor must be capable of sensing small rotations; at 0.2 Hz, the sensitivity requirement is 3×10^{-9} rad/ $\sqrt{\text{Hz}}$. A laser-based optical ring gyroscope, operating on the Sagnac principle, is currently being developed. Counter propagating beams will be locked to a triangular cavity using Pound-Drever-Hall locking. The rotation rate of the ring can be determined through the feedback signal used to lock the cavity. We report here on the current status and progress of this project.

Contents

1	Introduction	4
2	Project Objectives	5
2.1	Background	5
2.2	Current Technology	5
3	Building a Passive Laser Gyroscope	6
3.1	Requirements	6
3.2	Design	6
3.3	Finesse	7
3.4	Sensitivity Limitations	7
4	Experimental Progress	8
4.1	Characterization of the NPRO Lasers	9
4.2	Divergence Measurements of the NPRO Lasers	10
4.3	Noise Measurements of 495 mW NPRO Laser	12
4.4	Simple Cavity Optical Setup	14
5	Schedule	15
6	References	16
Appendix A		
	Pound-Drever-Hall Locking	17

1. Introduction

Gravitational waves were first predicted as a consequence of Einstein's General Theory of Relativity. These “ripples in space-time” are quadrupole emissions given off in response to the change in position of some massive astronomical bodies, such as binary neutron stars or black holes, and propagate through space at the speed of light. The Laser Interferometry Gravitational-wave Observatory (LIGO) is a collaboration of more than 600 scientists whose goal is to detect these gravitational waves [1].

Three main detectors comprise LIGO. Two of these are collocated in Hanford, Washington, one with 4 km arms and a second inside of it with 2 km arms, although the 2 km detector is not currently being used. The third 4 km detector is located in Livingston, Louisiana [1]. Having detectors in different locations is necessary in order to confirm the event of a gravitational wave detection, and to be able to locate the region of the sky from which the source originated [2]. The detectors operate as Michelson interferometers, and a simple conceptual model for the way they work is this: if a gravitational wave passes by, one arm will be stretched while the other will be contracted, and this relative motion between the test-mass mirrors at the end of each arm will cause a change in the interference pattern at the output.

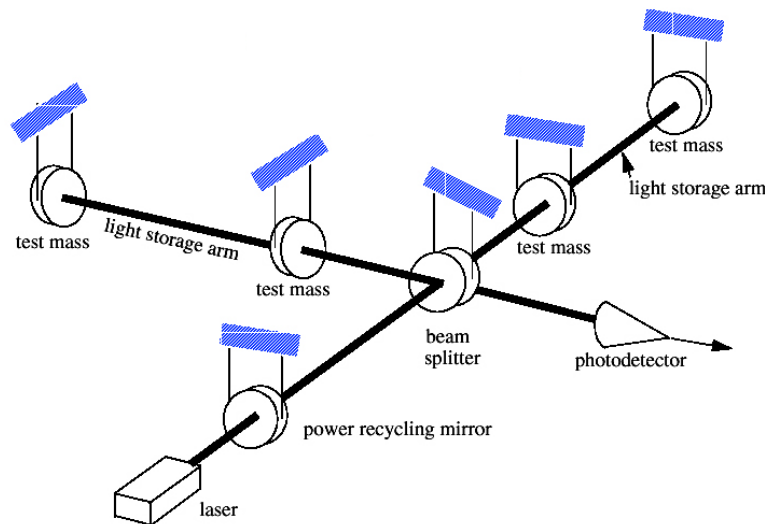


Fig. 1. Diagram including the main components of the LIGO interferometers [3].

Initial LIGO first took data in 2002, and has had five science runs since that time. In November of 2005, at the beginning of the fifth science run, Initial LIGO reached its design sensitivities, however, noise still dominated the signal, and to-date no gravitational waves have been detected [3]. Advanced LIGO is a planned upgrade to the detectors which will increase sensitivity by a factor of about 10, and will listen to a volume of space 1,000 times greater than that of Initial LIGO [4]. Much of the ongoing work in LIGO is focused on decreasing the various noise sources in the detectors, such as seismic noise arising from the motion of the ground, thermal noise in the mirrors, laser intensity (radiation pressure) noise, and shot noise. Together, the radiation pressure and the shot noise comprise quantum noise. Decreasing the shot noise involves increasing the laser intensity, which increases the radiation pressure. In this way, there is a fundamental limit to the quantum noise called the Standard Quantum Limit.¹ Advanced LIGO ultimately aims to be limited by quantum noise.

¹ It is possible for the detectors to operate below the Standard Quantum Limit by using ‘squeezed’ states of light. For a further discussion of this, see A. Heptonstall’s “Characterization of Mechanical...” p.22 [6].

The consequences of being able to detect gravitational waves are tantalizing. Scientists would be capable of seeing a huge volume of the universe that is currently dark to us, and could observe the most energetic events happening in it. The processes that continue to form the structure of our universe – mergers of black holes, supernovae – could be seen in an entirely different spectrum. We may even see things that are unfathomable and unpredictable from our current perspective. Much like the advent of radio or infrared astronomy, gravitational wave observatories will be a whole new window into understanding the cosmos.

2. Project Objectives

2.1 Background

One of the major noise sources in the LIGO detectors is due to the motion of the earth's crust – from things like seismic activity, tidal deformation, and simply cars driving on nearby freeways. Advanced LIGO's test masses will be suspended as pendulums from 400 μm quartz fibers, which are as strong as steel. This takes advantage of an interesting property of pendulums: at frequencies above their resonant frequency the pendulums are very effective at filtering out ground motion. Above resonance, the motion of the test masses falls off as $1/f^2$ [5]. It is at and below the resonant frequency of the pendulum that displacement of the test masses becomes problematic.

Seismometers at the detector sites are capable of measuring the motion of the ground very accurately, and they feed this signal forward to hydraulic HEPI actuators, which then make corrections for this motion. This system is good enough to achieve design sensitivity at frequencies above 10 Hz. At very low frequencies, however, ground tilt is coupled into the horizontal seismometer signal, which may cause the HEPI actuators to make erroneous corrections. Thus, some way of subtracting out this rotation component is necessary to reduce the noise in the detectors at low frequencies. This will also help with detector stability, reducing the gain needed to keep them locked. This in turn will make the detector more sensitive at higher frequencies. The focus of this project is to build a laser-based optical gyroscope capable of sensing ground tilt very accurately.

2.2 Current Technology

Laser-based gyroscopes operate on the Sagnac principle, where the path lengths for counter-propagating beams traveling around a rotating ring are different, yielding a beat frequency at the output of the cavity that is proportional to the rotation rate.

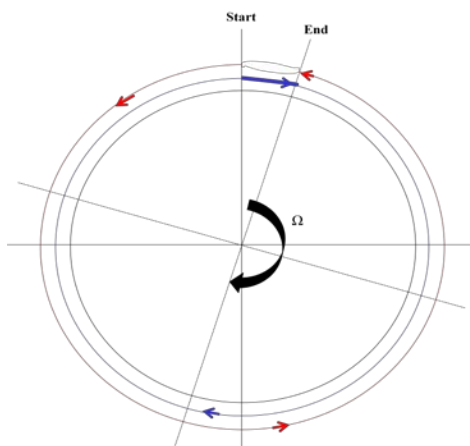


Fig. 2. Illustration of the Sagnac Effect

Because the output signal of a Sagnac interferometer is proportional to the relative speed of the test masses rather than their position, Sagnac interferometers are capable of operating below the Standard Quantum Limit [5].

Laser gyroscopes are commonly used in inertial guidance systems for military applications, and in some consumer items. These, however, are generally required to measure large, fast rotations, and do not require the high sensitivity that we need.

3. Building a Passive Laser Gyroscope

3.1 Requirements

For a horizontal seismometer, the ratio of sensitivity to rotation to sensitivity to horizontal motions at frequency ω is given by [6]:

$$\frac{\text{rotation sensitivity}}{\text{horizontal sensitivity}} = -\frac{g}{\omega^2}$$

To find the required sensitivity to rotations, it will be assumed that noise from the rotation sensor can contribute only 1/10th of the total noise in the horizontal direction. This will ensure that the seismometer's signal is not dominated by tilt, and the HEPI actuators will not make erroneous corrections. This can be expressed as [6]:

$$\Omega_{\text{sensitivity}} = \frac{1}{10} \frac{\omega^2}{g} x_{\text{sensitivity}}$$

Where $x_{\text{sensitivity}}$ is the horizontal sensitivity requirement. At 0.2 Hz, this gives a rotational sensitivity requirement of 3×10^{-9} rad/ $\sqrt{\text{Hz}}$.

3.2 Design

We are not as limited by the size constraints that commonly accompany units used in other applications. Our research is focused on a passive setup (the lasing medium is outside the cavity) using fixed mirrors.

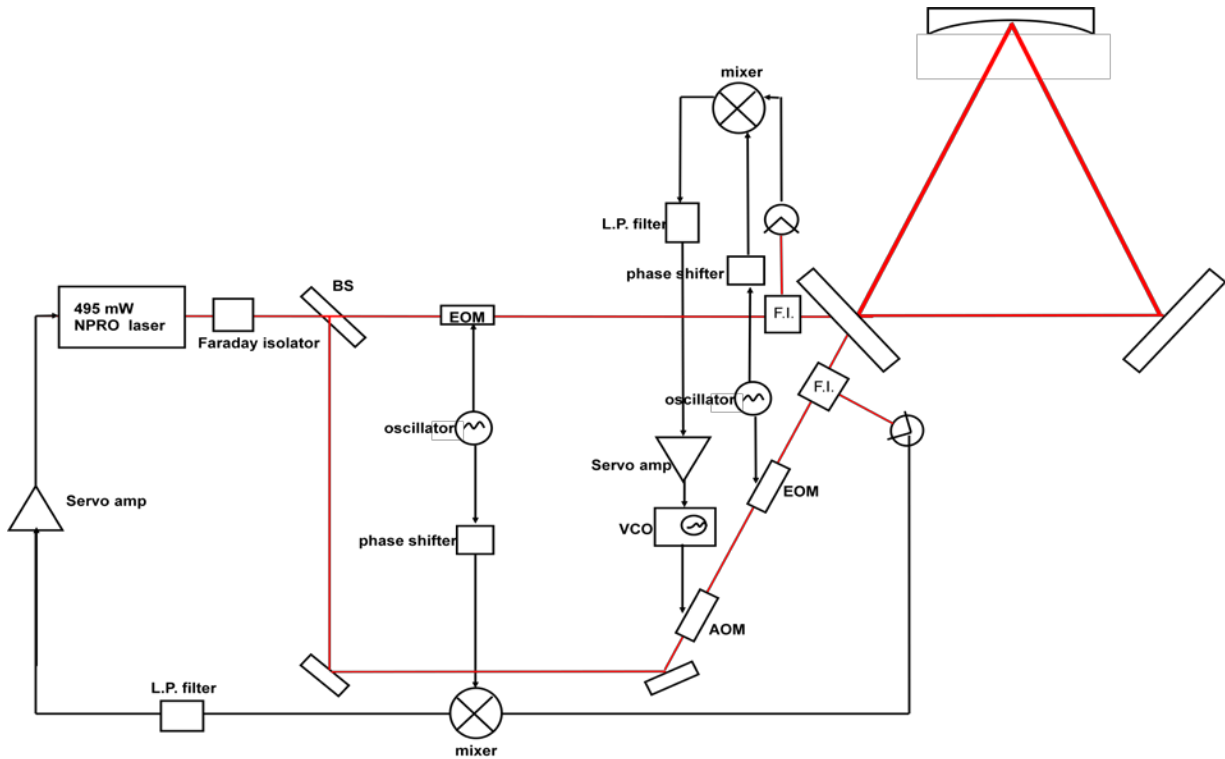


Fig. 3. Diagram of an externally excited passive laser gyroscope.

1064 nm light from a 495 mW NPRO laser will be split into two counter propagating beams, which will each be locked to the cavity using the Pound-Drever-Hall locking method.² Both beams will be modulated using an Electro-Optic Modulator (EOM) to produce sidebands, which allow the lasers to be locked. The sidebands are reflected from the cavity, acting as stable references that sample the phase of the main carrier. Thus, the EOM modulation frequency must not be resonant with the cavity. Each side of the triangular cavity will be 1 m in length, giving a free spectral range³ of 50 MHz. We will modulate the EOMs at 10 MHz.

The counterclockwise beam will be locked to the cavity by acting directly on the laser to alter its frequency. The clockwise beam will then be locked to the counterclockwise mode, using an Acousto-Optic Modulator (AOM) to alter its frequency.

Our readout point will be the modulation frequency of the AOM, which is proportional to the rotation rate of the ring.

3.3 Finesse

The finesse of the cavity is completely determined by the losses in the mirrors, where $1 - \rho$ is lost on each round trip, according to:

$$\mathcal{F} = \frac{\pi}{2 \sin^{-1} \left(\frac{1 - \sqrt{\rho}}{2\sqrt{\rho}} \right)}$$

A higher finesse means lower energy loss in the cavity. It is also inversely proportional to the full width at half-maximum bandwidth of the cavity resonances, with a proportionality constant equal to the free spectral range of the cavity. Thus, a higher finesse denotes a smaller range of frequencies at which the laser will resonate in the cavity, and in our system, results in a more stable laser.

The triangular cavity consists of two mirrors with a reflectance of 99.99% and one partially transmitting mirror with a reflectance of 99 ± 0.5 %. This yields a finesse of approximately 1000. The high reflectance mirrors have reflective coatings that can be damaged if the intensity incident on them is too high. CVI specifies that the coatings can handle 0.5 MW/cm^2 for a continuous-wave laser. Estimating that the beam on the mirrors will have approximately a 1 mm diameter, this gives a maximum permissible power of 3.93 MW. We will not, then, have to worry about the mirror coatings limiting the finesse, at least initially. If we find the need for a higher finesse in the future, we may need to change the mirrors or the coatings, in which case we may have to consider how the damage threshold of the mirrors will limit the finesse.

3.4 Sensitivity Limitations

While the error signal is a measurement of laser frequency noise, it is not possible to distinguish between this, and length noise in the cavity. Length noise in the cavity can be reduced by using stable

² See appendix for discussion of the Pound-Drever-Hall Technique

³ The free spectral range is defined as the frequency spacing between successive resonant modes in a cavity. It is given by $\Delta\nu = c/2L$, where c is the speed of light and L is the length of the resonator.

optical mounts for the mirrors [7]. The whole system is being locked on resonance, so the carrier is not reflected. Because of this, variation in the laser power, the modulation amplitude, and the modulation frequency do not contribute to the error signal [8]. Fluctuations in the sideband power will contribute to the error signal, however, this effect falls off as the frequency increases [9].

We expect a few other sources to contribute to noise in the error signal, including the vibrations of mirrors and thermal expansion of the optical table. Ultimately, however, we expect that our laser gyroscope will be limited in sensitivity by shot noise. The sensitivity of a shot noise-limited passive laser gyroscope is given by [10]:

$$\delta\Omega = \frac{\lambda P}{4A} \frac{\sqrt{2}\Gamma}{\sqrt{(n_{ph}\eta\tau)}}$$

Where P is the perimeter of the ring, A is the area enclosed therein, Γ is the full width at half maximum bandwidth, n_{ph} is the number of photons arriving at the detector, η is the detector efficiency, and τ is the integration time. For a cavity with 1m sides, a finesse of 1000, and the maximum power output of our laser, the sensitivity will be 2.5×10^{-8} rad/ $\sqrt{\text{Hz}}$.

Say the power incident on the mirrors is held constant. We can then explore how the shot noise-limited sensitivity scales with the finesse of the cavity, using the above expression.

$$\delta\Omega \propto \Gamma$$

where it is understood that all other parameters are fixed. But finesse can also be written as

$$\mathcal{F} = \frac{\Delta\nu}{\Gamma}$$

where $\Delta\nu$ is the free spectral range of the cavity (see footnote on previous page). Thus,

$$\delta\Omega \propto \frac{\Delta\nu}{\mathcal{F}}$$

It is clear from this expression that the uncertainty in measuring the rotation rate of the ring decreases as the finesse increases, or the sensitivity scales directly with finesse.

4. Experimental Progress

Before proceeding with the design of the laser gyro, we are focused on building and locking a simple Fabry-Perot cavity using Pound-Drever-Hall techniques. When we add the third mirror for the triangular cavity, we will already have a working control system, and a working modulation and demodulation system.

While working on the alignment of the Fabry-Perot cavity, we discovered that our 495 mW NPRO laser's diode was overheating, and causing the laser to shut down. We are currently investigating the cause of this overheating, and in the meantime we will be using a 1 W NPRO laser. This laser is housed in the same lab as our experiment, and is shared with an experiment working on fiber noise

cancellation. We use a beam splitter and half wave plates to independently control the power going into each experiment. This is not a permanent solution, however, since both experiments need to independently frequency-stabilize the laser.

4.1 Characterization of the NPRO Lasers

The output power as a function of drive current for each laser was measured. The results were plotted in Matlab, and error bars denote the range over which the power fluctuated during a period of approximately 30 seconds. Plots for each laser are shown in figures 4 and 5.

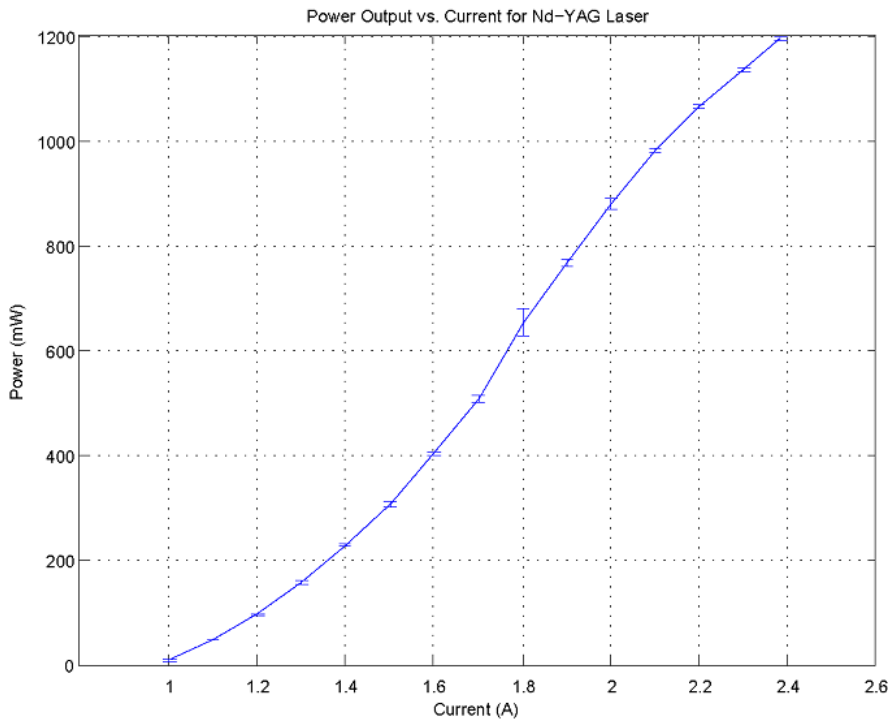


Fig. 4. Power output for 1 W laser.

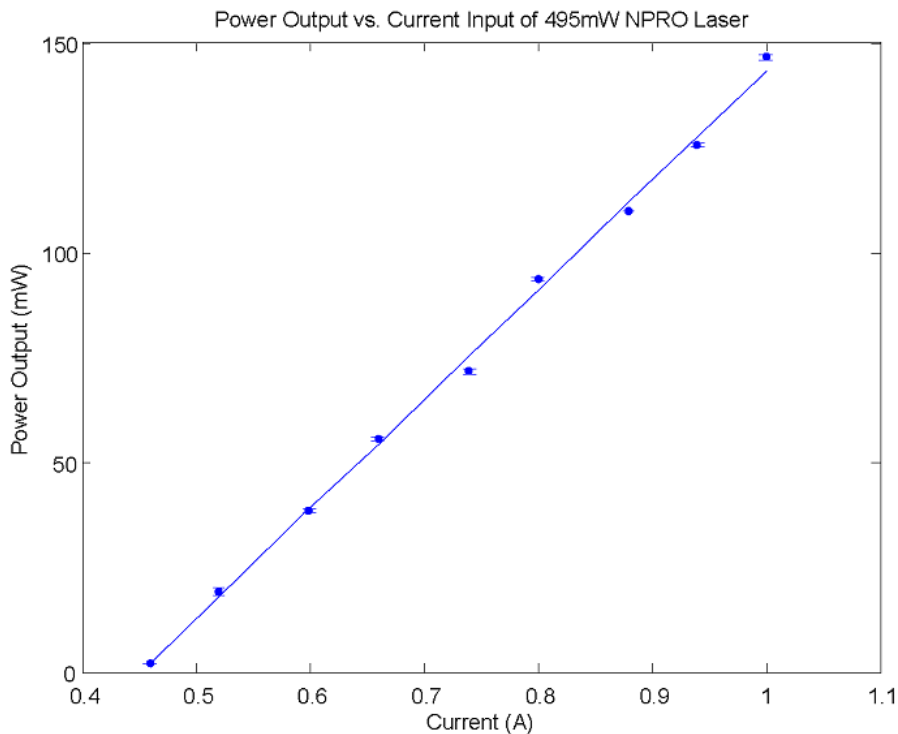


Fig. 5. Power output for 495 mW laser. Error bars are very small, indicating a fluctuation of just a few milliwatts at each measured current.

4.2 Divergence Measurements of the NPRO Lasers

Both lasers operate in the fundamental transverse mode and have a Gaussian profile. Gaussian beams diverge with distance according to [11]:

$$w(z) = w_0 \sqrt{\left(1 + \left(\frac{\lambda z}{\pi w_0^2}\right)^2\right)}$$

where w_0 is the half-width of the beam at its narrowest point, called the *waist*, and $w(z)$ is the half-width of the beam at a distance z from the waist, as shown in the figure below.

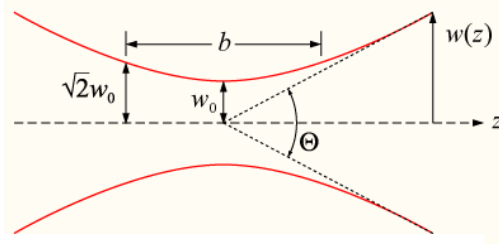


Fig. 6. Contour of a Gaussian beam.

The asymptotes in figure 4 correspond to [11]:

$$\Theta = \frac{\lambda}{\pi w_0}$$

where a small angle approximation has been made. It is necessary to know how the beam of our laser diverges, so that we can avoid diffraction losses in the cavity and the other optics of our setup by correctly refocusing the beam.

Measurements were taken using a BeamScan XYS-10A, which profiles the beam along two perpendicular axes. The full widths at which the intensities drops to $1/e^2(I_{\max})$ were found as a function of distance from the lasers' apertures. The data were plotted using Matlab.

For the 1 W NPRO, it was found that the beam's divergence was linear, suggesting that it had reached its asymptotic value. It is likely that the output coupler of the laser just before the aperture causes this rapid divergence. The size of the beam's waist was found by measuring the slope of the data, and approximating it as Θ . The characteristic divergence was then fit to the data by using a least-squares linear regression in Matlab. The waist was found to be virtual, and located behind the housing of the laser. The results of this are shown in figure 7.

For the 495 mW NPRO, we found that the data was non-linear, suggesting that we had taken data both near the waist of the beam and where the divergence became linear. The same fitting procedure was applied and the results are shown in figure 8. Unlike the 1 W NPRO, this laser's waist is real and located in front of the aperture.

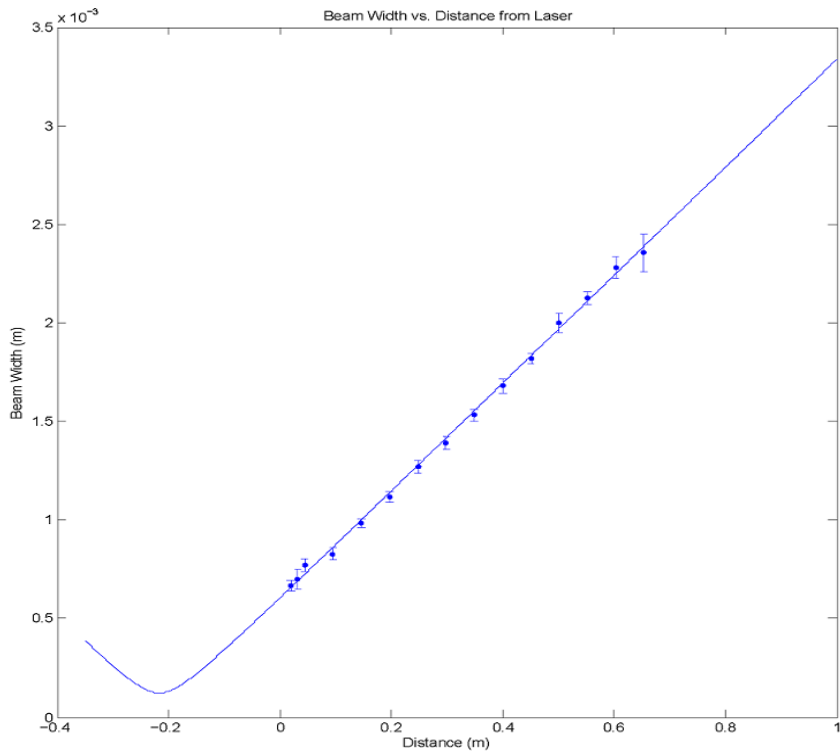


Fig. 7. Beam divergence of a 1 W Nd-Yag laser. The waist is located 21.5 cm behind the laser aperture, with a half-width of 124 micrometers.

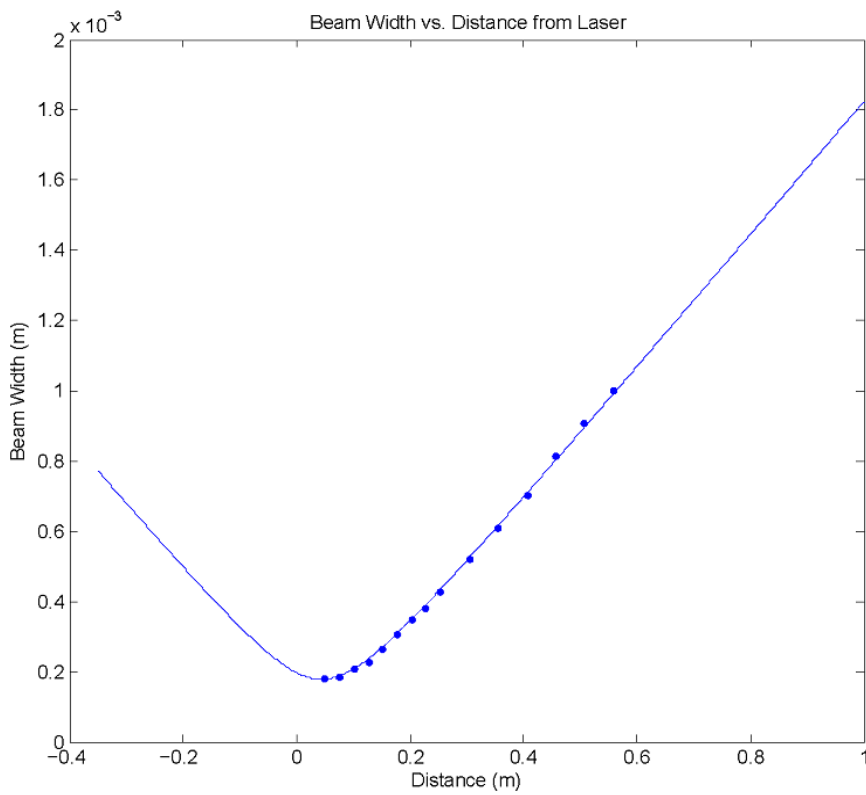


Fig. 8. Beam divergence of a 495 mW Nd-Yag laser. The waist is located 4.6 cm in front of the laser aperture, with a half-width of 178 micrometers.

4.3 Noise Measurements of the 495 mW NPRO

An SRS Spectrum Analyzer was used in parallel with an oscilloscope to measure various sources of noise in the 495 mW NPRO laser. The beam was sent into a PDA10CS photodetector, and that signal was fed to the spectrum analyzer and oscilloscope. The electronics noise was first measured with no power incident on the photodetector, and then the total noise at 2 mW, 4 mW, 7 mW, and 9 mW was measured. Data from the spectrum analyzer was saved to disk, and Matlab was used to plot it. This information allows for the determination of the intensity noise at each of these powers. A theoretical calculation for shot noise was also done, the derivation of which is shown on the next page.

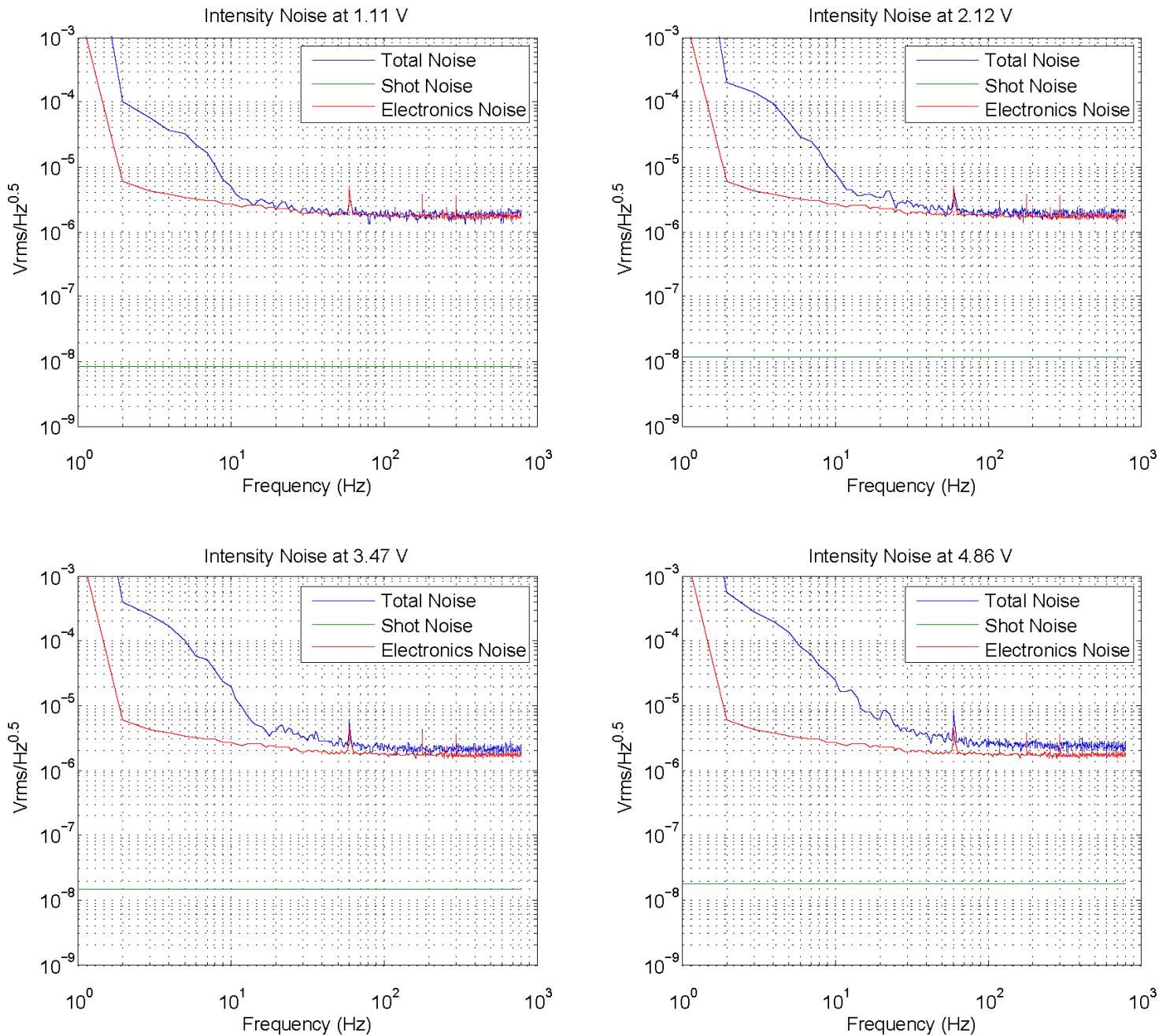


Fig. 9. Amplitude spectral density measurements of 495 mW NPRO laser taken at 4 different power levels.

Light is not incident on the photodetector as a continuous stream of energy, but rather as a patter of photons. The quantum shot noise limit arises statistically because we are counting photons. It is well known that the uncertainty in counting these photons goes as the square root of the number of photons incident on the detector, that is to say:

$$\sigma N_{ph} = \sqrt{N_{ph}}$$

where N_{ph} is the number of photons incident on the detector and σ is used here and throughout the rest of the derivation to indicate an uncertainty. In practice, however, we do not actually count photons. Thus, we must convert this to some useful, measurable quantity. The photodetector converts whatever power is incident on it into an electronic signal; a voltage. This is measurable, so we will use the above expression to find an expression for the uncertainty in the measured voltage.

$$N_{ph} = \frac{P_o \tau}{h\nu} = \frac{P_o \tau}{E}$$

The number of photons can be written in terms of the power incident on the photodetector, P_o , the energy per photon, E , and the integration time, τ . The above two relations then yield an uncertainty in measuring E :

$$\sigma E = \sqrt{h\nu P_o \tau}$$

In order to obtain a voltage from this, we must take advantage of two parameters specific to the photodetector: its gain, and its responsivity. The former is measured in units of V/A, and the latter is measured in units of A/W. For the Thorlabs PDA 10CS model that we used, the gain was 0.75×10^3 V/A, and the responsivity was 0.7 A/W. Using this, we discover that

$$\sigma I = (\sigma E)R$$

where σI is the uncertainty in current, and R is the responsivity of the photodetector. From there, it is easy to see that

$$\sigma V = (\sigma I)G$$

Where G is the gain of the photodetector, and σV is the quantity we are looking for, the uncertainty in the voltage. From this, it is also clear that shot noise should have a flat profile, and indeed this is what we see on the plots.

One step in the derivation was left ambiguous, that is, how to determine P_o ? This is the purpose of using an oscilloscope in parallel with the spectrum analyzer. We can determine the voltage from the photodetector directly from the oscilloscope, and work backwards to find the power incident on the photodetector. This relationship is

$$P_o = \frac{V}{GR}$$

4.4 Simple Cavity Optical Setup

Before beginning to set up and lock the triangular cavity, we will try to lock a simple cavity using Pound-Drever-Hall.⁴ This setup is in the process of being aligned. It is shown with its components labeled in the image below.

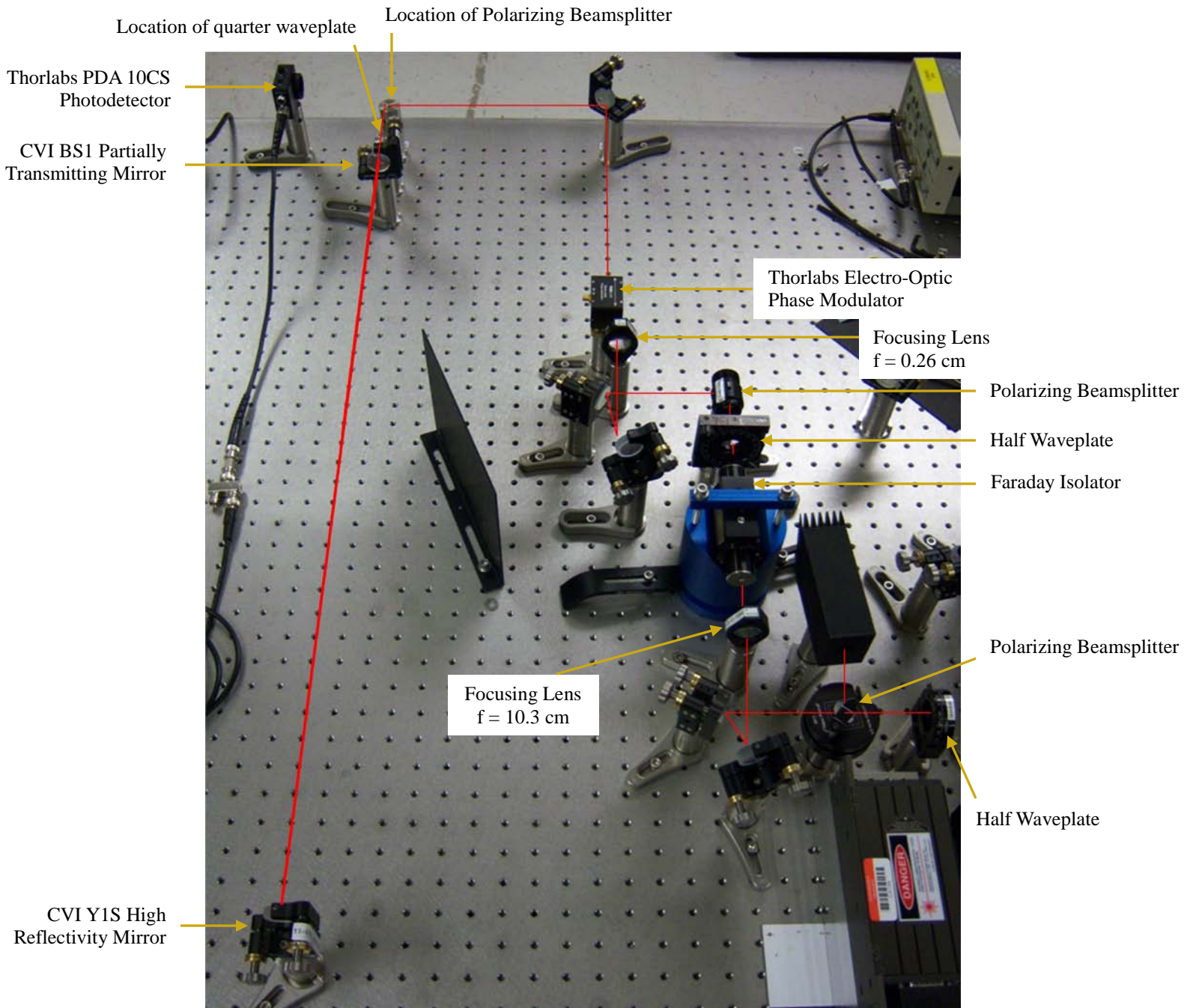


Fig. 10. Initial setup of a Fabry-Perot cavity for Pound-Drever-Hall locking.

⁴ The setup for this is shown schematically in Appendix A.

The length of the Fabry-Perot cavity is 0.71 m, yielding a free spectral range of 210 MHz (see footnote on page 7). The EOM will be driven at 8 MHz so the sidebands will not be on resonance with the cavity. Not shown in the picture above is the function generator which drives the EOM. The output of the photodetector is mixed with the signal from the function generator, and this new signal is sent through a 1 MHz low pass filter, through a servo amp, and back to the laser. This completes the feedback loop by altering the laser's frequency to match the cavity length.

5. Schedule

Below is the original timetable for the project.

1.5 Weeks	Theory and calculations
2 Weeks	Ordering/making parts
2 Weeks	Locking a simple cavity
2 Weeks	Setting up/locking the triangular cavity
2.5 Weeks	Troubleshooting

The problems with the 495 mW NPRO and various other things have set us behind schedule. The EOM has proved difficult to align. Its aperture is just 2 mm, and it is located in the middle of the optics bench very near a focusing lens. This makes it difficult to center the beam on the aperture, even with the aid of an infrared viewer. The polarization of the beam also needed to be changed upon exiting the Faraday Isolator. The EOM crystal's extraordinary axis is vertical (normal to the optics bench), and the beam coming from the Faraday Isolator is rotated 45 degrees with respect to this. The purpose of the half wave plate and polarizing beamsplitter at the output of the Faraday Isolator is to change this polarization angle. We should finish locking the simple cavity by the end of this coming week, at which point we can begin setting up the triangular cavity.

6. References

- [1] B. Barish and R. Weiss. LIGO and the Detection of Gravitational Waves. *Physics Today*, 44-50. Oct. 1999.
- [2] Saulson, Peter. *Fundamentals of Interferometric Gravitational Wave Detectors*. World Scientific Publishing Co., 1994.
- [3] A. Weinstein. SURF Lectures, 2009. <http://www.ligo.caltech.edu/~ajw/LIGO_SURF09.pdf>.
- [4] Cadonati. "Listening to Space with LIGO."
http://www.ligo.caltech.edu/~ajw/IntroPapers/cadonati_06.pdf
- [5] A. Heptonstall. *Characterization of Mechanical Loss in Fused Silica Ribbons for Use in Gravitational Wave Detector Suspensions*. Doctoral Thesis, University of Glasgow, 2004.
- [6] A. Heptonstall et al., *Optical Gyroscopes for Ground Tilt Sensing in Advanced LIGO*, G0900270-x0.
- [7] R. Adhikari. *Sensitivity and Noise Analysis of 4 km Laser Interferometric Gravitational Wave Antennae*, P040032-00-D.
- [8] E. Black. *Notes on the Pound-Drever-Hall Technique*, T980045-00-D.
- [9] E. Black. *An introduction to Pound-Drever-Hall frequency stabilization*, *Am. J. Phys.* 69 (1), January 2001.
- [10] G. A. Sanders et al., *Passive ring resonator method for sensitive inertial rotation measurements in geophysics and relativity*, *Optics Letters* 6 (1981) 11.
- [11] H. Kogelnik and T.Li. *Laser Beams and Resonators*, *Applied Optics* 5 (1966) 10.

Appendix A. Pound-Drever-Hall Locking

Pound-Drever-Hall locking [8, 9] is a technique used in several parts of the LIGO detectors because it is a very fast feedback mechanism and produces a very frequency-stable laser. “Locking” in this context refers to either altering a laser’s frequency to be an integer multiple of a cavity’s free spectral range, or altering the length of the cavity to match the laser’s frequency. We will be utilizing the former of these two techniques, and a simple schematic diagram of this is shown below.

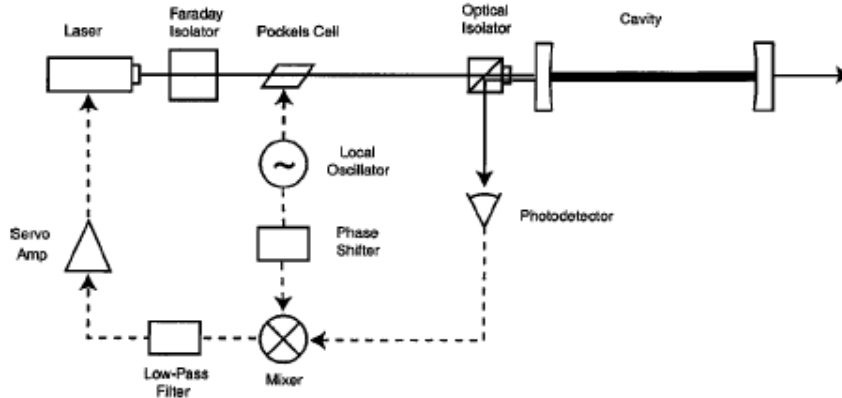


Fig. 11. Setup for locking a laser to a cavity [9]

This system is set up in such a way that it will hold the reflected intensity at zero; hence, it will keep the laser’s frequency on resonance with the cavity. Although the reflected intensity is symmetric about resonance, this system samples the derivative of the reflected intensity. This is done by dithering the frequency and gauging the response of the reflected beam. In the setup above, the frequency is modulated with a Pockels Cell, which is labeled as an EOM in our setup. The Pockels Cell is modulated at a known frequency with the local oscillator. The reflected beam is sent to the photodetector via an optical isolator. The signal from the local oscillator and the photodetector are mixed, and the output contains a low frequency (dc) signal, and a signal at twice the modulation frequency. The dc signal is what samples the derivative of the reflected intensity, thus a low-pass filter is placed between the mixer and the servo amp which will feedback to the laser. The phase shifter in the diagram is used in practice to compensate for unequal delays in the signal paths, since we need to mix two sinusoids which are in phase with each other.

Below is the characteristic error signal of Pound-Drever-Hall locking. The error signal is linear near resonance, allowing any change in the frequency to be compensated for.

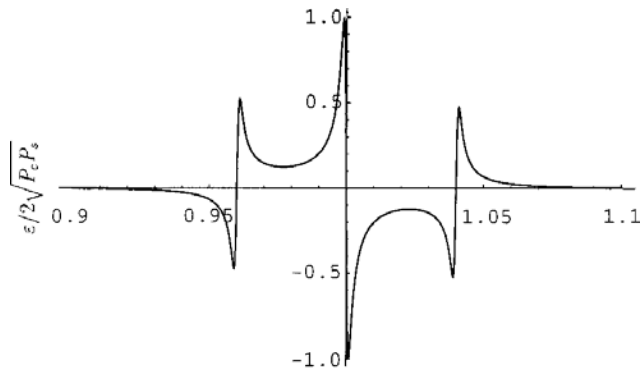


Fig. 12. The Pound-Drever-Hall error signal [9]